Neuroendocrine Gene Expression Coupling of Interoceptive Bacterial Food Cues to Foraging Behavior of *C. elegans*

Sonia A. Boor[1,2], Joshua D. Meisel[2,3], Dennis H. Kim[1,*]

1. Division of Infectious Diseases, Department of Pediatrics, Boston Children's Hospital and Harvard Medical School, Boston, MA 02115
2. Department of Biology, Massachusetts Institute of Technology, Cambridge, MA 02139
3. Department of Molecular Biology, Massachusetts General Hospital, Boston, MA 02114

* Correspondence to dennis.kim@childrens.harvard.edu

The authors declare no competing interests.

Author contributions:

SAB: Conceptualization, Formal analysis, Validation, Investigation, Visualization, Methodology, Writing—original draft, Writing—review and editing

JDM: Investigation, Visualization, Writing – review and editing

DHK: Conceptualization, Supervision, Funding acquisition, Visualization, Methodology, Writing—original draft, Writing—review and editing

Summary

Animal internal state is modulated by nutrient intake, resulting in behavioral responses to changing food conditions. The neural mechanisms by which internal states are generated and maintained are not well understood. Here, we show that in the nematode *Caenorhabditis elegans,* distinct cues from bacterial food – interoceptive signals from the ingestion of bacteria and gustatory molecules sensed from nearby bacteria – act antagonistically on the expression of the neuroendocrine TGF-beta ligand DAF-7 from the ASJ pair of sensory neurons to modulate foraging behavior. A positive-feedback loop dependent on the expression of *daf-7* from the ASJ neurons acts to promote transitions between roaming and dwelling foraging states and influence the persistence of roaming states. SCD-2, the *C. elegans* ortholog of mammalian Anaplastic Lymphoma Kinase (ALK), which has been implicated in the central control of metabolism of mammals, functions in the AIA interneurons to regulate foraging behavior and cell-non-autonomously control the expression of DAF-7 from the ASJ neurons. Our data establish how a dynamic neuroendocrine *daf-7* expression feedback loop regulated by SCD-2 functions to couple sensing and ingestion of bacterial food to foraging behavior. We further suggest that this neuroendocrine feedback loop underlies previously characterized exploratory behaviors in *C. elegans*. Our data suggest that the expression of *daf-7* from the ASJ neurons contributes to and is correlated with an internal state of "unmet need" that regulates exploratory foraging behavior in response to bacterial cues in diverse physiological contexts.

Introduction

Internal states, such as fear, arousal, and hunger, are shaped by the integration of information about internal and external conditions and can result in the modulation of various

physiological and behavioral outputs (Flavell et al., 2022). As animals encounter different food environments, information about internal nutritional status and external food quality can elicit transitions between internal states that either favor the exploration of new places or exploitation of the current environment. Many animals, including mammals, zebrafish, *Drosophila melanogaster*, and the roundworm *Caenorhabditis elegans,* increase exploration in response to food deprivation in order to increase chances of a food encounter (Ben Arous et al., 2009; Connolly, 1966; Gutman et al., 2007; Herbers, 1981; Johnson et al., 2020; Overton & Williams, 2004; Russell et al., 1987). However, the mechanisms behind how animals couple changes in food availability to internal states that influence foraging behavior are not well understood. Insight into the cellular and organismal mechanisms governing internal states may enhance understanding of the dysregulation of internal states that is thought to contribute to many human psychiatric and neurological diseases (Flavell et al., 2022; Yap & Greenberg, 2018).

C. elegans forage for microbes that grow on decaying organic matter, where they encounter fluctuations in not only the quantity of nutritious bacterial food available but also in the quality and pathogenicity of this bacterial food (Kim & Flavell, 2020). As they navigate their food environments, *C. elegans* exhibit two-state foraging and feeding behavior known as roaming and dwelling (Ben Arous et al., 2009; Flavell et al., 2013; Flavell et al., 2020; Fujiwara et al., 2002). On abundant nutritious food, animals spend about 80% of their time dwelling and 20% of their time roaming; as food becomes scarcer or lower in quality, animals increase the proportion of their time roaming (Ben Arous et al., 2009). The internal states that underlie *C. elegans* roaming and dwelling responses to changing food conditions present an experimentally tractable paradigm in which to study how internal states are regulated. Furthermore, the shared modulators of internal states and high degree of genetic conservation between *C. elegans* and

65 humans suggest that understanding *C. elegans* feeding and foraging behavior could have relevant
66 implications for human health and disease.

67 Aided by a complete connectome (White et al., 1986), a growing body of work has
68 examined neural circuits and their effects on foraging behavior in *C. elegans* (Ji et al., 2021;
69 Pradhan et al., 2019). The excitation or inhibition of neurons in these circuits elicits rapid
70 behavioral modulation as well as persistent behavioral states through recurrent neuronal firing.
71 Neuronal dynamics are additionally influenced by neuromodulators (Bargmann, 2012).
72 Neuromodulators play a key role in mediating internal states by functioning at titratable levels
73 over longer timescales and farther distances than direct synaptic signaling (Flavell et al., 2022;
74 Sengupta, 2013). For instance, the activation of a small group of neurons can induce transitions
75 between roaming and dwelling states through conserved serotonin and pigment dispersing factor
76 signaling (Flavell et al., 2013; Ji et al., 2021). Other neuromodulators such as dopamine and
77 octopamine can further influence foraging behavior and food-dependent locomotion (Churgin et
78 al., 2017; Oranth et al., 2018; Sawin et al., 2000). Activity-dependent gene expression in neurons
79 has been established to have key roles in the development and plasticity of neuronal circuits, but
80 less is known about how changes in neuronal gene expression may shape internal states driving
81 behavior (Yap & Greenberg, 2018). As transcription occurs on a slower timescale than neuronal
82 firing or neuromodulator release, dynamic gene expression could be important in regulating the
83 persistence of internal states.

84 We have been studying the dynamic temporal and neuron-specific expression of *daf-7*,
85 which encodes a TGF-beta ligand that is involved in the neuroendocrine regulation of a diverse
86 range of behaviors in *C. elegans*, including the dauer developmental decision, longevity,
87 metabolism, and feeding and foraging behavior (Ben Arous et al., 2009; Greer et al., 2008; Ren

et al., 1996; Schackwitz et al., 1996; Shaw et al., 2007). Expression of *daf-7* is restricted to a limited set of sensory neurons, including the ASI neurons (Meisel et al., 2014; Ren et al., 1996; Schackwitz et al., 1996). DAF-7 expression from the ASI neurons was shown to respond to changing environmental conditions, such as crowding and food levels (Entchev et al., 2015; Ren et al., 1996; Schackwitz et al., 1996). Previously, we observed that highly dynamic *daf-7* expression can be observed in the ASJ neurons, with induction of expression in response to secondary metabolites produced by pathogenic *Pseudomonas aeruginosa* PA14, which is necessary for pathogen avoidance behavior (Meisel et al., 2014). In addition, we have shown that upon the onset of reproductive maturity, male *C. elegans* upregulate *daf-7* expression in their ASJ neurons to promote male mate-searching behavior (Hilbert & Kim, 2017).

Here, we have identified that the ingestion of bacterial food regulates the expression of a single gene in two neurons to shape internal state dynamics driving foraging behavior in *C. elegans*. We observed that *daf-7* transcription levels in the ASJ neurons couples foraging behavior to changes in bacterial food ingestion, under the control of the highly conserved receptor tyrosine kinase SCD-2/ALK. The relationship between gene transcription and behavioral states across organisms is largely uncharacterized (Yap & Greenberg, 2018), and our results establish SCD-2/ALK-regulated dynamic *daf-7* expression as a gene-expression correlate and driver of internal states underlying foraging behavior in response to changing nutritional conditions.

Results

Ingested food inhibits *daf-7* expression in the ASJ neurons

110 Our lab has previously reported that when adult hermaphrodites are fed the normal *E. coli*
111 OP50 food source, *pdaf-7::GFP* expression is restricted to the ASI chemosensory neurons
112 (Hilbert & Kim, 2017; Meisel et al., 2014). In contrast, we observed that when animals were fed
113 OP50 treated with aztreonam, an antibiotic that causes the bacteria to form inedible long strands
114 (Gruninger et al., 2008), *pdaf-7::GFP* was expressed in both the ASI and ASJ neurons (Figures
115 1A, 1C, 1D). These data suggested that ingestion of food inhibits *daf-7* expression in the ASJ
116 neurons. However, we did not observe *daf-7* expression in the ASJ neurons in the complete
117 absence of food ("Empty"), which indicated that some bacterial component of non-ingestible
118 aztreonam-treated *E. coli* OP50 was required for the induction of *daf-7* in the ASJ neurons in the
119 absence of ingested food (Figures 1A, 1C, 1D). The non-ingestible food signal that results in the
120 upregulation of *daf-7* expression in the ASJ neurons on aztreonam-treated food could be
121 diffusible, volatile, or mechanosensory. To identify the nature of the non-ingestible food cue, we
122 exposed animals to food that had been seeded on the lid of the plate (exposing animals to only
123 the volatile food cues) ("Lid") or underneath the agar (exposing animals only to diffusible food
124 cues) ("Bottom") in the absence of ingestible food and probed *daf-7* expression. We observed
125 induction of *daf-7* in the ASJ neurons when OP50 is seeded under the agar of the plates, but not
126 when present on the lid of the plate, suggesting that a bacteria-derived food signal that diffuses
127 through the agar is necessary for the induction of *daf-7* expression in ASJ in the absence of
128 ingested food. (Figures 1A-F). Thus, these data suggest that in hermaphrodites feeding on *E. coli*
129 OP50, there is an external water-soluble diffusible cue from the bacteria that stimulates *daf-7*
130 expression from the ASJ neurons, but this expression is inhibited by a second bacteria-derived,
131 interoceptive cue generated from the ingestion of bacteria (Figure 1B).

132 We next asked whether the inhibition of *daf-7* expression in the ASJ neurons by ingestion
133 of bacterial food was mediated by the early detection of ingested food or the delayed nutritional
134 effects of bacterial food consumption on organismal physiology. The kinetics of *pdaf-7::GFP*
135 induction in the ASJ neurons when animals were moved from ingestible to non-ingestible food
136 showed a rapid upregulation within 2-3 h for the GFP fluorescence in the ASJ neurons to become
137 visible (Figure 1G). Given the delay for GFP folding and accumulation to visible levels, these
138 data suggested that the absence of ingested food rapidly led to the induction of *daf-7* expression
139 in the ASJ neurons. Recent work has described the interoceptive sensing of ingested food by the
140 acid-sensing ion channels (ASICs) encoded by *del-3* and *del-7*, which are expressed in the minor
141 neurites of the NSM neurons where they detect food in the pharynx and mediate behavioral
142 slowing upon encountering food (Rhoades et al., 2019). We observed that *del-3;del-7* animals
143 have elevated expression *daf-7* in the ASJ neurons on ingestible food but show wild-type levels
144 of *daf-7* expression on non-ingestible food or no food (Figure 1H). These observations are
145 consistent with the hypothesis that the detection of an interoceptive ingested food signal in the
146 pharynx, mediated by DEL-3 and DEL-7, inhibits *daf-7* expression in the ASJ neurons.
147

148 ***daf-7* expression in the ASJ neurons promotes roaming behavior**

149 Next, we sought to understand how changes in *daf-7* expression in the ASJ neurons in
150 response to changing food conditions might modulate food-dependent behavior. Feeding *C.*
151 *elegans* alternate between two distinct behavioral states known as roaming and dwelling (Ben
152 Arous et al., 2009; Fujiwara et al., 2002). On nutritious food, wild-type animals spend most of
153 their time dwelling, a feeding state marked by a low movement speed and high body bending
154 angle. As food conditions worsen, animals will decrease the fraction of time dwelling and

155 increase the fraction of time roaming, a foraging state marked by high speed and low curvature
156 (Ben Arous et al., 2009). Prior analysis of roaming and dwelling has identified that animals
157 increase the proportion of time roaming on aztreonam-treated food, and genetic analysis has
158 revealed a role for DAF-7 in promoting roaming behavior, with *daf-7* animals spending a
159 decreased fraction of time roaming compared to wild-type animals (Ben Arous et al., 2009).
160 Using both worm-tracking software to quantify roaming and dwelling (*WormLab*, 2020) and an
161 exploration assay to measure the general activity levels of animals ((Flavell et al., 2013), see
162 Materials and Methods), we observed that *daf-7(e1372)* and *daf-7(ok3125)* animals spent a
163 markedly decreased proportion of time in the roaming state than wild-type animals, consistent
164 with these prior findings (Figure 2A). To determine whether we could detect modulation of
165 roaming and dwelling behaviors caused by changes in *daf-7* expression in the ASJ neurons, we
166 adopted two complementary approaches. First, we found that in a *daf-7(ok3125)* background,
167 rescue of *daf-7* cDNA under the ASJ-specific *trx-1* promoter partially restored the fraction of
168 time animals spent in the roaming state (Figure 2B). Second, we examined exploratory behavior
169 in animals that had *daf-7* deleted in the ASJ neurons, using a floxed allele of *daf-7* and Cre
170 expressed under the *trx-1* promoter. We found that animals with an ASJ-specific *daf-7* deletion
171 explored less of the lawn and spent less time roaming than animals with wild-type expression of
172 *daf-7* (Figure 2C).

173 The relationships between ingested food and *daf-7* expression in the ASJ neurons, *daf-7*
174 expression in the ASJ neurons and roaming, and roaming and amount of food ingested suggest a
175 neuroendocrine gene expression positive-feedback loop that couples the ingestion of bacterial
176 food to the modulation of foraging behavior through *daf-7* expression in the ASJ neurons (Figure
177 2D). When animals are on abundant edible food, the ingestion of this food inhibits *daf-7*

178 expression in the ASJ neurons and attenuates the proportion of time in the roaming state. When
179 animals are removed from edible food but are still exposed to soluble food signals, upregulation
180 of *daf-7* expression in the ASJ neurons promotes an increased proportion of time in the roaming
181 state. Considering that animals can exist in one of the two states while feeding on bacterial food,
182 a decreased fraction of time roaming could be due to shorter roaming states, longer dwelling
183 states, or combination of these factors. We hypothesized that this transcriptional feedback loop
184 might function in the persistence of internal states underlying roaming and dwelling behaviors,
185 so we measured the duration of roaming and dwelling states in animals lacking DAF-7 signaling.
186 Representative trace files of wild-type, *daf-7(e1372),* and *daf-7(ok3125)* animals show
187 how DAF-7 can influence roaming and dwelling state duration (Figure 2E). Quantification of
188 state duration across multiple animals revealed that *daf-7* animals exhibited shortened roaming
189 states relative to wild-type animals as predicted by the positive feedback loop (Figure 2F). We
190 did not observe a difference in dwelling state duration among the genotypes examined, although
191 we suspect the wide variation dwelling state durations exhibited by animals precluded the
192 detection of a statistically significant difference with our analysis.
193
194 **Neuromodulatory mechanisms that affect foraging behavior alter *daf-7* expression in the**
195 **ASJ neurons**
196 The positive-feedback loop supported by our data (Figure 2D) suggests a correlation
197 between *daf-7* expression in the ASJ neurons and genetic backgrounds favoring roaming
198 behavior and hence a diminished ingestion of bacterial food. Serotonin has been shown to
199 promote long dwelling states, and thus animals with mutations in *tph-1,* the gene encoding the
200 enzyme that catalyzes the rate-limiting step of serotonin biosynthesis, spend a greater proportion

201 of their time in the roaming state (Figure 3A) (Flavell et al., 2013; Ji et al., 2021). Consistent
202 with the correlation between *daf-7* expression in the ASJ neurons and roaming, we see that *tph-*
203 *1(n4622)* animals constitutively express *daf-7* in the ASJ neurons on ingestible food, no food,
204 and non-ingestible food, with this *daf-7* expression retaining sensitivity to changes in food
205 environments (Figure 3B). These results suggest that serotonin signaling may influence *daf-7*
206 expression in parallel to the gustatory and interoceptive food cues.

207 Pigment dispersing factor (PDF) signaling has also been previously shown to modulate
208 roaming and dwelling behavior, with animals carrying loss-of-function mutations in the PDF
209 receptor gene *pdfr-1* showing a decreased fraction of their time in the roaming state than wild-
210 type animals (Figure 3C) (Flavell et al., 2013; Ji et al., 2021). Consistent with the correlation
211 between roaming and *daf-7* expression in ASJ, we observed that animals with loss-of-function
212 mutations in *pdfr-1* do not upregulate *daf-7* transcription in the ASJ neurons on non-ingestible
213 food (Figure 3D). From a screen done in parallel to this work, we recovered a putative gain-of-
214 function allele of *pdfr-1*, *pdfr-1(qd385),* carrying a S325F substitution (Boor, 2022). Follow-up
215 analysis in an independently generated S325F allele*, pdfr-1(syb3826)*, confirmed that this
216 substitution was responsible for our observed phenotypes. We observed that *pdfr-1(syb3826)*
217 animals exhibited increased roaming behavior compared with wild-type animals (Figure 3C) and
218 constitutive expression of *daf-7* in the ASJ neurons in the presence of ingestible food, which was
219 further upregulated under conditions of no bacterial food or non-ingestible food (Figure 3D).
220 These results are consistent with a model in which PDFR-1 signaling influences *daf-7* expression
221 in the ASJ neurons by modulating the sensation of the external gustatory food cue.
222

223 **SCD-2 controls *daf-7* expression in the ASJ neurons and roaming**

224 To identify additional genetic factors involved in coupling the ingestion of food to *daf-7*
225 expression in the ASJ neurons and its subsequent effect on roaming, we were guided by the
226 isolation of an allele of *hen-1, hen-1(qd259),* from a screen we previously performed for genes
227 regulating the expression of *daf-7* from the ASJ neurons in response to *P. aeruginosa* (Park et
228 al., 2020). Through genomic rescue experiments, we confirmed that the *hen-1* mutation was the
229 causative lesion in this strain, and animals with mutations in *scd-2,* encoding the receptor of
230 HEN-1, share this phenotype (Figure 4A). SCD-2 has characterized for its role in the food-
231 dependent developmental arrest known as dauer diapause and sensory integration (Reiner et al.,
232 2008; Shinkai et al., 2011; Wolfe et al., 2019), and Anaplastic Lymphoma Kinase (ALK), the
233 human ortholog of SCD-2, has been implicated in metabolic phenotypes in humans, mice, and
234 *Drosophila* (Orthofer et al., 2020). Taken together, these observations led us to question if SCD-
235 2 might be involved in the regulation of *daf-7* expression in the ASJ neurons in response to
236 changes in food ingestion. We found that animals with loss-of-function alleles of *scd-2* showed
237 reduced upregulation of *daf-7* in the ASJ neurons in response to non-ingestible food compared to
238 wild-type animals, implicating SCD-2 at least partially in this *daf-7* expression response (Figure
239 4B).
240 To further examine the role of SCD-2 mediating the *daf-7* expression response to
241 ingested food, we generated a gain-of-function allele. Gain-of-function point mutations in ALK
242 are associated with neuroblastoma and most often occur in the kinase domain, with 85% of all
243 ALK point mutations seen at either F1174 or R1275 (Franco et al., 2013). F1174L, the most
244 common point mutation, results in ALK autophosphorylation and cytokine-independent growth
245 (Chen et al., 2008; George et al., 2008; Hallberg & Palmer, 2013; Holla et al., 2017; Janoueix-
246 Lerosey et al., 2008). Analysis of a sequence alignment of SCD-2 and ALK revealed that F1174

247 in ALK was conserved as F1029 in SCD-2, and we were able to create a gain-of-function allele
248 of *scd-2* by engineering a F1029L substitution (*scd-2(syb2455)*) (Figure 4C) (Boor, 2022). To
249 infer whether SCD-2 activity was sufficient to induce expression of *daf*-7 in the ASJ neurons in
250 the absence of ingestible bacterial food, we examined the gain-of-function *scd-2(syb2455)*
251 mutant and observed that these animals constitutively expressed *daf-7* in the ASJ neurons even in
252 the presence of ingestible food (Figure 4B). We further observed that the magnitude of
253 upregulation of *daf-7* expression in the ASJ neurons when animals were moved from ingestible
254 food to non-ingestible food was reduced in *scd-2(syb2455)* to levels only about one-fifth of that
255 seen in wild-type animals (the ratio of wild-type *daf-7* expression in the ASJ neurons on non-
256 ingestible food to ingestible food = 8.1; the ratio of *scd-2(syb2455) daf-7* expression in the ASJ
257 neurons on non-ingestible food to ingestible food = 1.7) (Figure 4B). In contrast to the reduced
258 upregulation seen in the *scd-2(syb2455)* gain-of-function animals when exposed to non-
259 ingestible food, *scd-2(syb2455)* exhibited robust upregulation of *daf-7* expression in the ASJ
260 neurons when exposed to *P. aeruginosa* (Figure 4A). The observation that this PA14-dependent
261 upregulation is intact in *scd-2(syb2455)* animals while the non-ingestible food-dependent
262 upregulation is attenuated supports a direct role for SCD-2 in the response to ingested food
263 rather than a global control of *daf-7* expression in the ASJ neurons.
264 Expression of *scd-2* cDNA under the AIA-specific *gcy-28.d* promoter has been shown to
265 be sufficient to rescue behavioral phenotypes of *scd-2* mutants that have been attributed to a role
266 for AIA-expressed SCD-2 in sensory integration (Shinkai et al., 2011; Wolfe et al., 2019). To ask
267 whether SCD-2 could be functioning in the AIA neurons to regulate *daf-7* expression in the ASJ
268 neurons, we generated a strain with the coding sequence of SCD-2 floxed and introduced a
269 transgene expressing Cre under the *gcy-28.d* promoter. Compared to animals containing a floxed

270 *scd-2* allele without Cre, animals with AIA-specific Cre expression resulting in AIA-specific
271 deletion of *scd-2* showed reduced upregulation of *daf-7* expression in the ASJ neurons in
272 response to non-ingestible food, suggesting that SCD-2 activity in the AIA neurons acts cell-non-
273 autonomously to control *daf-7* expression in the ASJ neurons (Figure 4D).

274 Our finding that SCD-2 regulates the *daf-7* expression in response to ingested food
275 predicts that SCD-2 would also promote roaming behavior. Consistent with this hypothesis, we
276 observed that animals with loss-of-function mutations in *scd-2* spent a lower proportion of time
277 roaming and explored less of the lawn in an exploration assay than wild-type animals (Figure
278 4E). Animals with a loss-of-function allele of *hen-1* also roamed less than wild type (Figure 4E).
279 Furthermore, as predicted by the regulation of *daf-7* expression in the ASJ neurons, *scd-2* and
280 *hen-1* animals exhibit shorter roaming states and unchanged dwelling state durations compared
281 to wild-type animals (Figure 4F). When we examined the roaming and dwelling behavior of *scd-*
282 *2(syb2455)* gain-of-function animals, we found that these mutants showed increased roaming
283 behavior and lawn exploration as compared to wild-type animals and exhibited longer roaming
284 states (Figure 4G and 4H). Consistent with SCD-2 mediating roaming partially through its
285 influence on *daf-7* expression in the ASJ neurons, we saw that the increased roaming exhibited
286 by *scd-2(syb2455)* animals was reduced in animals with a Cre-lox-mediated ASJ-specific *daf-7*
287 deletion (Figure 4I). As with the regulation of *daf-7* expression in the ASJ neurons, we observed
288 that Cre-lox-mediated deletion of *scd-2* specifically in the AIA neurons reduced both roaming
289 and exploration compared to floxed *scd-2* animals without Cre, suggesting that SCD-2 functions
290 in the AIA interneurons to promote roaming behavior (Figure 4J).

291

292 **A neuronal gene expression correlate of internal state dynamics driving foraging behavior**

293 Considering our positive feedback model, we reasoned that conditions under which we
294 have observed *daf-7* expression in the ASJ neurons would correlate with increased roaming
295 behavior. Previous work from our lab has shown that upon reaching reproductive maturity, male
296 *C. elegans* induce *daf-7* expression in their ASJ neurons, which contributes to male mate-
297 searching behavior (Figure 5A) (Hilbert & Kim, 2017). Consistent with the behaviors that have
298 been reported for males and hermaphrodites in bacterial food-leaving assays (Lipton et al.,
299 2004), we observed that wild-type males spend a greater proportion of their time in the roaming
300 state than hermaphrodites (Figure 5B). We also observed that the *daf-7* expression in the ASJ
301 neurons in males was sensitive to the inhibitory effects of ingested food, although the magnitude
302 of the fold increase in *daf-7* expression from the ASJ neurons was about half that observed for
303 hermaphrodites (Figure 5A).
304 We have also previously reported an upregulation in *daf-7* expression in the ASJ neurons
305 when animals are on pathogenic *P. aeruginosa* PA14 in response to specific secondary
306 metabolites phenazine-1-carboxamide and pyochelin (Figure 5C) (Meisel et al., 2014). Analysis
307 of roaming and dwelling on PA14 revealed that animals significantly increase the fraction of
308 their time in the roaming state on PA14 compared to nonpathogenic *E. coli* OP50 (Figure 5D).
309 We observed that upon exposure to the nonpathogenic PA14 mutant ΔgacA, which results in an
310 intermediate level of *daf-7* expression in the ASJ neurons (Figure 5C) (Meisel et al., 2014),
311 animals roamed an intermediate amount between animals on OP50 and pathogenic PA14 (Figure
312 5D).
313
314 **Discussion**
315

316 **A neuroendocrine gene expression feedback loop couples the ingestion of bacterial food to**
317 **foraging behavior**

318 The data we present here support a model in which bacterial food ingestion regulates
319 roaming and dwelling behavior in part via SCD-2-dependent *daf-7* expression in the ASJ
320 neurons. Our identification of the AIA neurons as the site of SCD-2 action is consistent with a
321 role for the AIA neurons in relaying food signals in other contexts. AIA has been characterized
322 as a downstream synaptic target of multiple food sensory neurons to integrate information about
323 the food environment and influence chemoreceptor expression in other neurons (Dobosiewicz et
324 al., 2019; McLachlan et al., 2022).

325 We have observed that the expression of *daf-7* in the ASJ neurons responds to two
326 opposing food cues. An interoceptive cue derived from the sensation of ingested food in the
327 pharynx inhibits the expression of *daf-7* in the ASJ neurons, while the presence of a diffusible
328 non-ingested food cue induces the expression of *daf-7* in the ASJ neurons (Figure 1B). In the
329 presence of both food cues, as on abundant ingestible food, the interoceptive food signal is
330 epistatic to the external food signal, promoting exploitation of the current food environment with
331 low levels of *daf-7* expression in the ASJ neurons. Our identification of two opposing food cues
332 is consistent with findings from Wexler et al., which reported that aztreonam-treated bacteria
333 could restore *daf-7* expression in the ASJ neurons of starved males, indicative of an external food
334 cue that is upregulating *daf-7* expression in the ASJ neurons (Wexler et al., 2020). Furthermore,
335 the activity of the ASJ neurons have been demonstrated to be modulated by removal of bacterial
336 supernatant (Zaslaver et al., 2015), consistent with ASJ responsiveness to an external food cue.

337 As discussed above, the relationship between foraging behavior, food ingestion, and
338 SCD-2-dependent *daf-7* expression has led us to posit a positive-feedback loop that couples food

339 ingestion with foraging behavior (Figure 2D). As animals in a patchy food environment
340 encounter a region with less edible food, our model predicts that a reduction of ingested food
341 would result in *daf-7* expression induction in the ASJ neurons via SCD-2. This increase in *daf-7*
342 expression is correlated with an internal state that favors roaming. As animals roam, they ingest
343 less bacteria, further promoting SCD-2-dependent *daf-7* expression in the ASJ neurons,
344 stabilizing a roaming-prone state. Once a roaming animal encounters edible food and begins to
345 eat, the interoceptive sensation of food in the pharynx results in a downregulation of *daf-7*
346 expression in the ASJ neurons, promoting a dwelling state in which the animal can continue to
347 eat. As additional food is ingested, this further reduces *daf-7* expression in the ASJ neurons,
348 stabilizing this internal state that favors dwelling. Moreover, a recent study has highlighted the
349 role of the ASJ neurons in promoting roaming and food-leaving behavior (Scheer & Bargmann,
350 2023). We additionally find that PDF and serotonin signaling appear to contribute to *daf-7*
351 expression in the ASJ neurons in addition to their previously characterized roles in roaming and
352 dwelling (Flavell et al., 2013; Ji et al., 2021).

353 A number of recent studies in *C. elegans* point to a key role for neuronal transcriptional
354 responses in the regulation of behavioral plasticity in response to changing environmental stimuli
355 such as food and temperature (Harris et al., 2023; Kyani-Rogers et al., 2022; Ryan et al., 2014;
356 Wexler et al., 2020). For example, differential expression of the diacetyl-sensing chemoreceptor
357 ODR-10 in the AWA neurons in response to changing food conditions, which functions
358 downstream of *daf-7* expression in the ASJ neurons of males, has been shown to modulate food-
359 leaving mate-searching behavior (Ryan et al., 2014; Wexler et al., 2020). We anticipate that the
360 characterization of neuron-specific transcriptional changes that are correlated with *daf-7*
361 expression in the ASJ neurons may yield additional mechanistic insights into how changing

362 environmental and endogenous ingested bacterial food levels modulate internal states driving
363 foraging behavior.
364
365 **SCD-2/ALK controls a neuroendocrine response to the ingestion of bacterial food**
366 Here, we show that *daf-7* expression in the ASJ neurons is regulated by the receptor
367 tyrosine kinase SCD-2. SCD-2 and its ligand, HEN-1, have been implicated sensory integration,
368 associative learning, and memory (Ishihara et al., 2002; Shinkai et al., 2011; Wolfe et al., 2019),
369 and SCD-2 was initially characterized for its role in regulating dauer formation, a
370 developmentally arrested state induced by stressful growth conditions, including lack of
371 nutritious food (Golden & Riddle, 1982, 1984a, 1984b, 1984c; Inoue & Thomas, 2000; Reiner et
372 al., 2008). SCD-2 is the *C. elegans* ortholog of Anaplastic Lymphoma Kinase (ALK). In humans,
373 *ALK* is expressed primarily in the nervous system and influences cell proliferation,
374 differentiation, and survival in response to external stimuli (Iwahara et al., 1997). Genetic
375 translocations resulting in gene fusions are common in *ALK*-dependent human cancers, including
376 non-small cell lung cancer (NSSLC), diffuse large B cell lymphoma (DLBCL), squamous cell
377 carcinoma (SCC), and renal cell carcinoma (RCC) (Hallberg & Palmer, 2013; Holla et al., 2017;
378 Morris et al., 1994). Recent studies have suggested a physiological role for ALK in the neuronal
379 control of metabolism. A genome-wide association study (GWAS) looking for genetic variants
380 associated with thinness identified a variant in the first intron of *ALK* (Orthofer et al., 2020).
381 Additional studies in *Drosophila* and mice have further implicated ALK in triglyceride
382 accumulation, starvation survival, and metabolic response to high-fat diets (Cheng et al., 2011;
383 Orthofer et al., 2020; Woodling et al., 2020).

384 We have observed a role for SCD-2 in regulating foraging behavior and neuroendocrine
385 gene expression in response to changing food conditions. We and others have observed that
386 animals with loss-of-function mutations in *scd-2* behave as if they are in the constant presence of
387 ingested "good" food; *scd-2* animals dwell more, reduce upregulation of *daf-7* expression in the
388 ASJ neurons in the absence of ingested food, and fail to enter dauer under poor food conditions
389 (Reiner et al., 2008). In contrast, animals with the gain-of-function *scd-2(syb2455)* allele act like
390 animals exposed to "bad" food conditions, as evidenced by increased roaming, constitutive
391 expression of *daf-7* in their ASJ neurons, and food-independent constitutive dauer entry (Boor,
392 2022). If SCD-2 is functioning in responding to changes in food, this may alter conclusions of
393 several previous studies implicating HEN-1 and SCD-2 in sensory integration, as several of the
394 assays employed in these studies have been shown to be affected by the animals' nutritional
395 status (Ishihara et al., 2002; Shinkai et al., 2011; Wolfe et al., 2019). Further investigation into
396 the role of SCD-2 in responding to food vs. sensory integration in these assays could be
397 informative.
398 Furthermore, the role for SCD-2 in regulating the physiological response to ingested food
399 in *C. elegans* is consistent with the growing body of work tying ALK and its orthologs to
400 thinness and metabolic phenotypes in humans, mice, and *Drosophila* (Cheng et al., 2011;
401 Orthofer et al., 2020; Woodling et al., 2020). Our observations of *scd-2 C. elegans* are consistent
402 with phenotypes seen in $ALK^{-/-}$ mice and *Alk* RNAi *Drosophila*, including increased energy
403 expenditure and reduced triglyceride accumulation (Orthofer et al., 2020). Since the phenotypes
404 of *scd-2* animals are associated with abundant food in *C. elegans,* we might expect these $ALK^{-/-}$
405 mice and *Alk* RNAi *Drosophila* to mimic animals that are constantly eating and engage in
406 compensatory mechanisms of increased energy expenditure and triglyceride metabolism. Further

407 characterization of the mechanisms by with SCD-2 and ALK regulate food-dependent behavior,
408 gene expression, and metabolism could reveal new factors governing body weight and have
409 implications in the treatment and prevention of obesity.
410

411 ***daf-7* expression in the ASJ neurons is correlated with an internal state favoring**
412 **exploration**

413 The response of *daf-7* expression in the ASJ neurons to changes in food conditions and
414 its effect on foraging behavior provides an example of the influence of gene expression on
415 internal states. We have identified a transcriptional switch of one gene in two cells that can
416 influence foraging behavior in a manner as equally simple as but on a longer time scale than
417 neuronal firing (Figure 5E). This *daf-7*-expressing, pro-roaming internal state might drive other
418 exploratory behaviors that our lab and others have observed under conditions were *daf-7* is
419 expressed in the ASJ neurons. Male *C. elegans* have been observed to upregulate the expression
420 of *daf-7* in their ASJ neurons upon reaching reproductive maturity, and this *daf-7* expression has
421 been implicated in driving mate-searching behavior (Hilbert & Kim, 2017). Males must find a
422 hermaphrodite mate to reproduce – a requirement not shared by hermaphrodites – and they often
423 must leave food to do so. The constitutive expression of *daf-7* in the ASJ neurons of adult males
424 could be due to a reduced sensitivity to ingested food allowing for prioritization of searching for
425 a mate over feeding. This is consistent with our observation that *daf-7* expression in the ASJ
426 neurons is upregulated less in response to non-ingestible food in males than in hermaphrodites.

427 Similarly, our lab has previously reported that two secondary metabolites of pathogenic
428 *P. aeruginosa* can result in the upregulation of *daf-7* expression in the ASJ neurons, which
429 contributes to pathogen avoidance behavior (Meisel et al., 2014). The results presented here

430 suggest that perhaps these secondary metabolites are tapping into this foraging circuit and
431 overriding other inputs that regulate *daf-7* expression in the ASJ neurons to promote the animals
432 moving away from the pathogen in a manner like roaming animals seeking nutritious food. In the
433 natural environment of *C. elegans*, pathogenic and nutritious bacteria coexist, and animals must
434 employ mechanisms to avoid infection while still obtaining adequate nutrition. Low levels of
435 nutritious food, the presence of pathogen, or an absence of mates each represents a suboptimal
436 environment and may induce a common internal state that promotes exploration and enhances
437 the chances of encountering more favorable conditions.

438 Multiple integrative neuronal mechanisms likely converge to establish "internal state"
439 that modulates organism behavior. Our data reveal that gene expression, specifically the
440 expression of a single gene, *daf-7*, from just two neurons, the ASJ chemosensory neurons, can
441 not only contribute to internal state driving foraging behavior through its role in a
442 neuroendocrine feedback loop, but also serve as a readily detected correlate of internal state
443 underlying foraging behavior.

444

445 **Materials and Methods**

446 ***C. elegans* strains:** *C. elegans* was maintained on *E. coli* OP50 as previously described
447 (Brenner, 1974). Daf-c strains were grown at 16˚C. See Table 1 for a complete list of strains used
448 in this study.

449 **Design of potential *scd-2* gain-of-function alleles:** We performed a protein alignment of *C.*
450 *elegans* SCD-2 and human ALK in NCBI BLAST (Figure 4C). Using a list of known oncogenic
451 ALK mutations (Holla et al., 2017), we screened these residues for conservation or similarity
452 between the *C. elegans* and human protein sequences. Genome editing was done by SunyBiotech

453 using CRISPR technology. Alleles were evaluated in a dauer assay for a gain-of-function Daf-c
454 phenotype, and validated in trans-heterozygote analysis with *scd-2(sa249)* for a dominant
455 phenotype (Boor, 2022).
456 **Preparation of food condition plates:** Unless otherwise indicated, all assays were performed on
457 NGM plates with no peptone. Aztreonam-treated bacteria was prepared as previously reported
458 (Gruninger et al., 2008), and 40 µL aztreonam-treated food was added to plates containing 10
459 µg/mL aztreonam. "Fed" plates for *daf-7* quantification were seeded with 40 µL OP50 grown
460 overnight in a shaking LB culture at 37˚C. "Bottom" plates were seeded with 250 µL OP50, and
461 the agar was inverted with a spatula immediately prior to adding animals. "Lid" plates were
462 prepared by pouring a spot of NGM agar on the inside of the lid of the plate and seeding 100 µL
463 of OP50 on to the spot. PA14 was grown as previously described and seeded onto SKA plates, as
464 were *E. coli* OP50 controls for these experiments (Meisel et al., 2014).
465 ***pdaf-7::gfp* quantification assays:** Plates of gravid animals were bleached and eggs were
466 dropped onto NGM plates seeded with OP50 and grown at 20˚C for 67 hours, unless otherwise
467 noted. On the day of imaging, 15-30 day one adult animals were transferred by picking to assay
468 plates, where they were incubated for 5 hours at 20˚C. Animals to be imaged were mounted on
469 glass slides with agarose pads and 50 mM sodium azide or 5 mM Levamisole. All imaging for
470 pictures were conducted on the Zeiss Axioimager Z1. Quantification of GFP brightness was
471 derived from maximum fluorescence values within the ASJ neurons in FIJI.
472 **Exploration assay:** The exploration assay was performed loosely as previously described with
473 several modifications (Flavell et al., 2013). Thirty-five millimeter NGM plates with no peptone
474 were seeded with 500 µL OP50 grown overnight in LB so that the lawn covered the entire
475 surface of the plate. On the day of the assay, one day-one adult animal was placed on the plate

476 and allowed to explore for two hours before being removed. The plate was then superimposed on
477 a grid of 3.5 mm squares and the number of squares crossed by the *C. elegans* tracks was
478 manually counted.
479 **Roaming/dwelling assay:** Animals were egg-laid and grown to day-one adults. 10 cm NGM
480 plates without peptone were seeded with 2 mL stationary phase *E. coli* OP50 grown overnight in
481 LB. Assays were performed with ~20 animals inside a 6 cm copper ring placed in the center of
482 the seeded plate. After one hour for the animals to adjust to their new environment, videos were
483 recorded at 3.75 frames per second for 1.5-3 hours. Videos were analyzed using MBF
484 Biosciences WormLab software (*WormLab*, 2020).
485 Measurements of speed and bending angle (midpoint) were averaged over 10 second
486 intervals, and values for each 10-second interval were plotted on a scatter plot of speed (µm/sec)
487 vs. bending angle (degrees). Quantification of fraction of time spent roaming or dwelling was
488 done by segregating the points of the scatter plots by a horizontal line whose placement was
489 based on the distribution of points in the control condition for each experiment. Values for this
490 speed cutoff ranged from y=7 to y=12. Points falling above the line were classified as roaming,
491 and those below the line were classified as dwelling. The fraction of time spent roaming was
492 calculated for each animal based off the speed cutoff. Outliers were removes using a ROUT test
493 with Q = 1%. The durations of roaming and dwelling states were determined manually by
494 analyzing average speed values for successive ten-second intervals. Only states lasting longer
495 than five intervals (fifty seconds) were considered.
496 **Statistics:** All statistical analysis was performed using the GraphPad Prism software (Graphpad
497 Prism, RRID: SCR_002798). Statistical tests used are indicated in each figure legend.
498

Acknowledgements: We thank Bob Horvitz, Steve Flavell, and the Caenorhabditis Genetics Center, which is funded by the NIH Office of Research Infrastructure Programs (P40 OD010440), for strains, and Cori Bargmann for Cre plasmids. We thank current and past members of the Kim lab for discussions. Finally, we acknowledge financial support from NIH grant R35GM141794.

Strain Name	**Genotype**	**Source**
N2	Wild type	Caenorhabditis Genetics Center (CGC)
JT249	*scd-2(sa249)*	CGC
RB783	*scd-2(ok565)*	CGC
JC2154	*hen-1(tm501)*	CGC
PHX2455	*scd-2(syb2455)*	This study/SunyBiotech
FK181	*ksIs2[pdaf-7::gfp; rol-6(su1006)]*	CGC
ZD2540	*ksIs2; scd-2(sa249)*	This study
ZD930	*ksIs2; scd-2(ok565)*	This study
ZD918	*ksIs2; hen-1(tm501)*	This study
ZD2605	*ksIs2; scd-2(syb2455)*	This study
CB1372	*daf-7(e1372)*	CGC
ZD715	*daf-7(ok3125)*	(Meisel et al., 2014)
ZD695	*daf-7(ok3125);qdEx34[ptrx-1::daf-7;pges-1::GFP]*	(Meisel et al., 2014)
ZD696	*daf-7(ok3125);qdEx35[ptrx-1::daf-7;pges-1::GFP]*	(Meisel et al., 2014)
ZD2632	*ksIs2; del-3(ok2613);del-7(ok1187)*	This study
MT14984	*tph-1(n4622)*	Horvitz Lab
ZD667	*ksIs2; tph-1(n4622)*	This study
ZD2079	*pdfr-1(ok3425)*	(Hilbert & Kim, 2018)
PHX3826	*pdfr-1(syb3826)*	This study/SunyBiotech
ZD1987	*ksIs2; pdfr-1(ok3425); him-5(e1490)*	(Hilbert & Kim, 2018)
ZD2633	*ksIs2; pdfr-1(syb3826); him-5(e1490)*	This study
ZD2721	*scd-2(syb5845 syb6052) Backcrossed x2*	This study
ZD2722	*daf-7(syb5855 syb5965) qdEx[ptrx-1::Cre; pofm-1::gfp] Backcrossed x2*	This study
ZD2752	*scd-2(syb5845 syb6052); ex[gcy-28.dp::cre; ofm-1p::gfp]*	This study

ZD2766	*scd-2(syb5845 syb6052); ex[gcy-28.dp::cre; ofm-1p::gfp]; ksIs2*	This study
ZD1005	*him-5(e1390); ksIs2*	(Hilbert & Kim, 2017)

506

507 **Table 1.** Complete list of *C. elegans* strains used in this study.

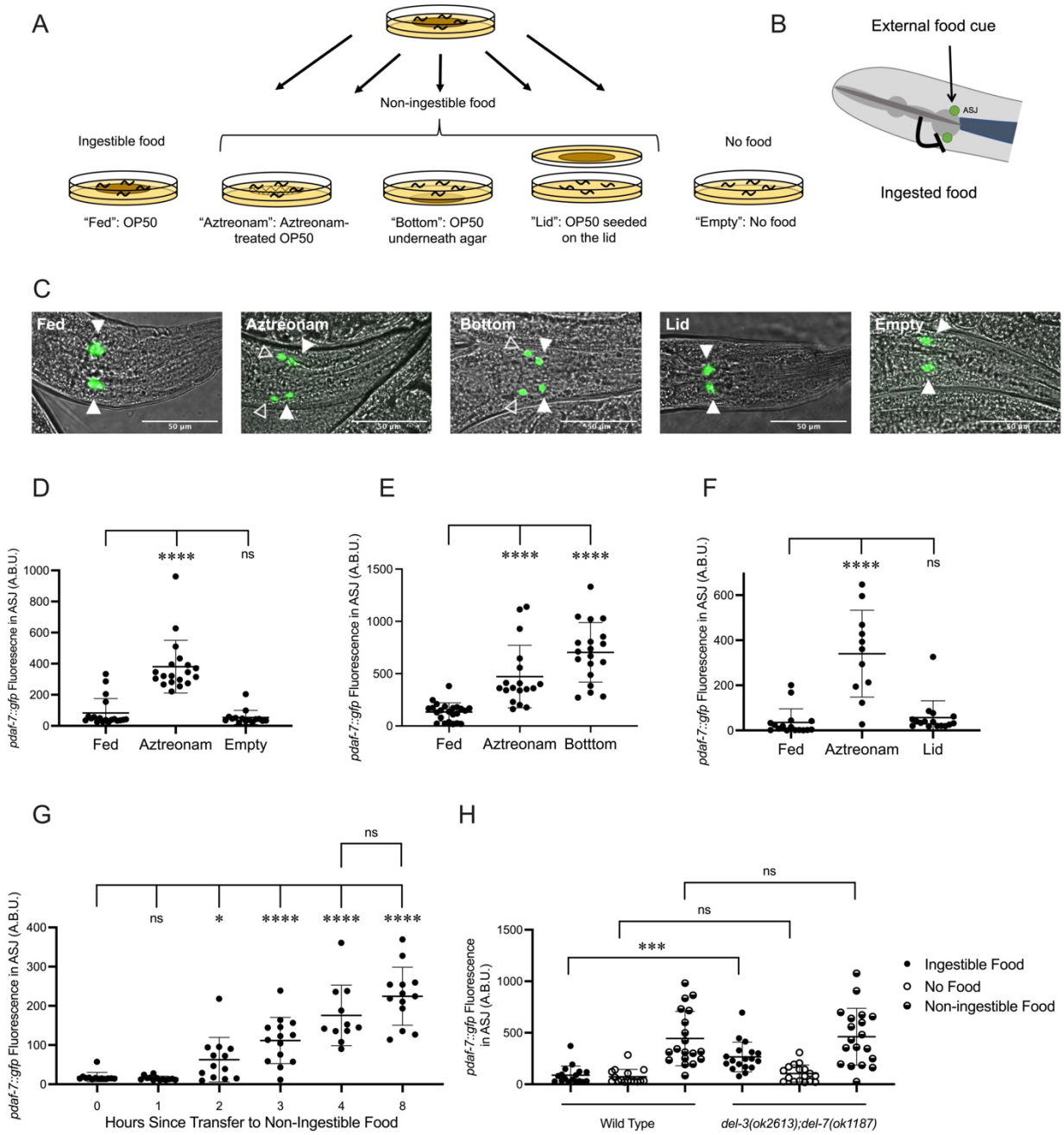

508

509 **Figure 1. Ingestion of bacterial food inhibits *daf-7* expression in the ASJ neurons.**

510 A. Schematic of experimental exposure to varied food conditions. Animals were grown to

511 adulthood on edible *E. coli* OP50, then transferred to various experimental food

512 conditions: "Fed": *E. coli* OP50; "Aztreonam": OP50 treated with aztreonam; "Bottom":

513 OP50 was seeded underneath the agar of the plate; "Lid": Animals placed on agar with

514 no food but where food was seeded on a spot of agar on the inside of the lid of the plate;
515 "Empty": no food.
516 B. Model for the convergence of external and ingested food signals on *daf-7* expression in
517 the ASJ neurons.
518 C. *pdaf-7::gfp* expression pattern in animals under different food conditions, from left to
519 right: "Fed," "Aztreonam," "Bottom," "Lid," "Empty." Filled triangles indicate the ASI
520 neurons; open triangles indicate the ASJ neurons. Scale bar indicates 50 µm.
521 D. E. F. Maximum fluorescence values of *pdaf-7::gfp* in the ASJ neurons of adult animals
522 under various food conditions. Each point represents an individual animal, and error bars
523 indicate standard deviation. ****$p<0.0001$, ns not significant as determined by an
524 unpaired two-tailed t-test.
525 G. Maximum fluorescence values of *pdaf-7::gfp* in the ASJ neurons of adult animals at
526 various time points after being moved from "Fed" to "Bottom" conditions. Each point
527 represents an individual animal, and error bars indicate standard deviation.
528 ****$p<0.0001$, * $p<0.05$, ns not significant as determined by an unpaired two-tailed t-
529 test.
530 H. Maximum fluorescence values of *pdaf-7::gfp* in the ASJ neurons of adult wild type and
531 *del-3(ok2613); del-7(ok1187)* under "Fed," "Bottom," and "Empty" conditions. Each
532 point represents an individual animal, and error bars indicate standard deviation.
533 ***$p<0.001$, ns not significant as determined by an unpaired two-tailed t-test.

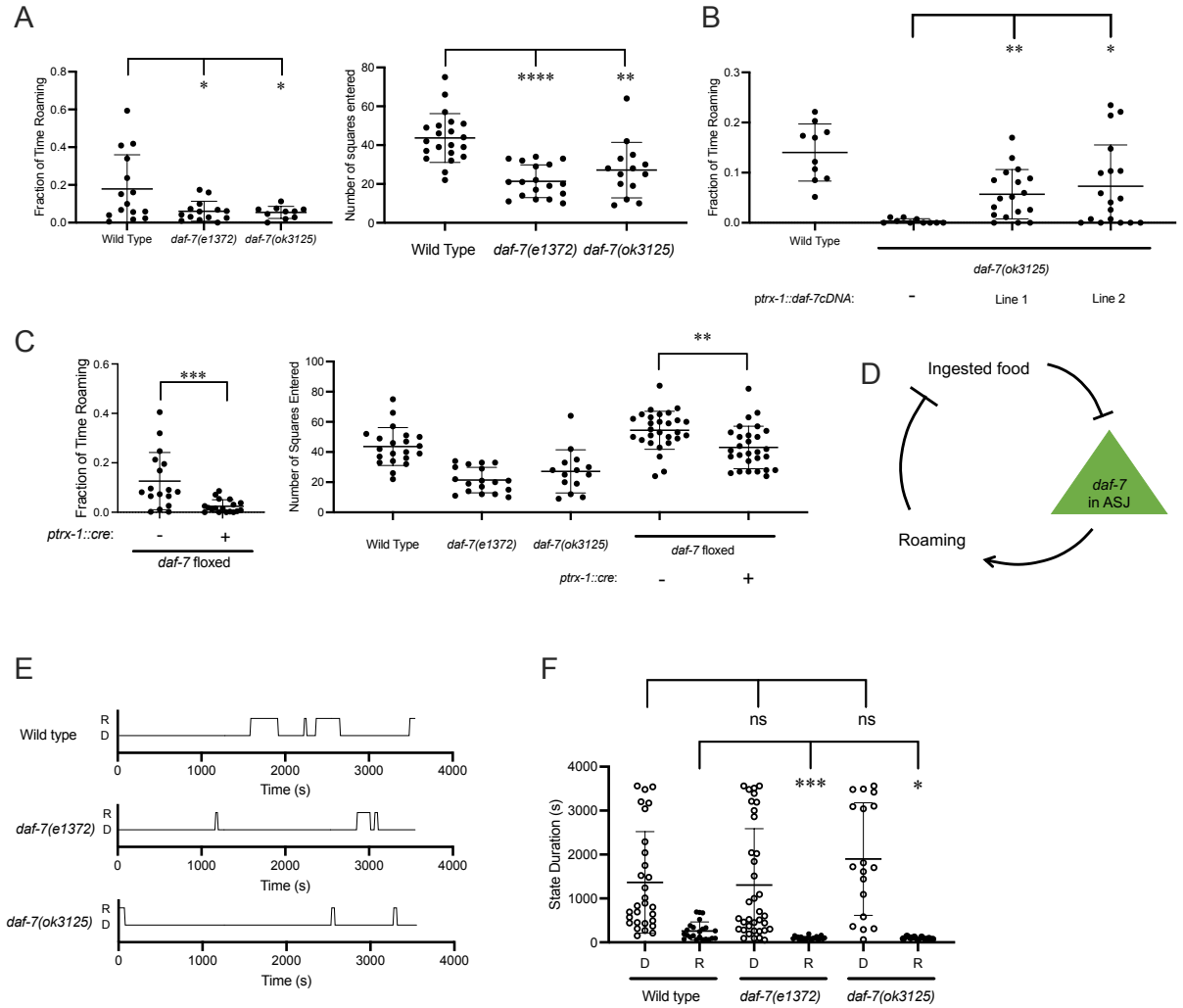

Figure 2. *daf-7* expression in the ASJ neurons promotes roaming.

A. Fraction of time roaming (left), and number of squares entered in exploration assay (right) of wild type, *daf-7(e1372)* and *daf-7(ok3125)* animals. Each point represents an individual animal, and error bars indicate standard deviation ****p<0.0001, **p<0.01, *p<0.05 as determined by an unpaired two-tailed t-test.

B. Fraction of time roaming of wild type, *daf-7(ok3125),* and two independent lines where *daf-7* cDNA was expressed under the *trx-1* promoter in a *daf-7(ok3125)* background. Each point represents an individual animal, and error bars indicate standard deviation. **p<0.01, *p<0.05 as determined by an unpaired two-tailed t-test.

545 C. Fraction of time roaming (left), and number of squares entered in exploration assay
546 (right) of wild type, *daf-7(e1372), daf-7(ok3125),* and a floxed *daf-7* strain with and
547 without Cre expressed under the *trx-1* promoter. Each point represents an individual
548 animal, and error bars indicate standard deviation. ** $p<0.01$, *$p<0.05$ as determined by
549 an unpaired two-tailed t-test.
550 D. Model of positive-feedback relationship between food ingestion, *daf-7* expression in the
551 ASJ neurons, and roaming.
552 E. Sample trace files of representative individual wild-type, *daf-7(e1372),* and *daf-*
553 *7(ok3125)* animals. R = roaming, D= dwelling.
554 F. Duration of dwelling (open circles) and roaming (closed circles) states for wild type, *daf-*
555 *7(e1372)* and *daf-7(ok3125)* animals. Each point represents a discrete roaming or
556 dwelling period. Error bars indicate standard deviation. ***$p<0.001$, *$p<0.05$, ns not
557 significant as determined by an unpaired two-tailed t-test.

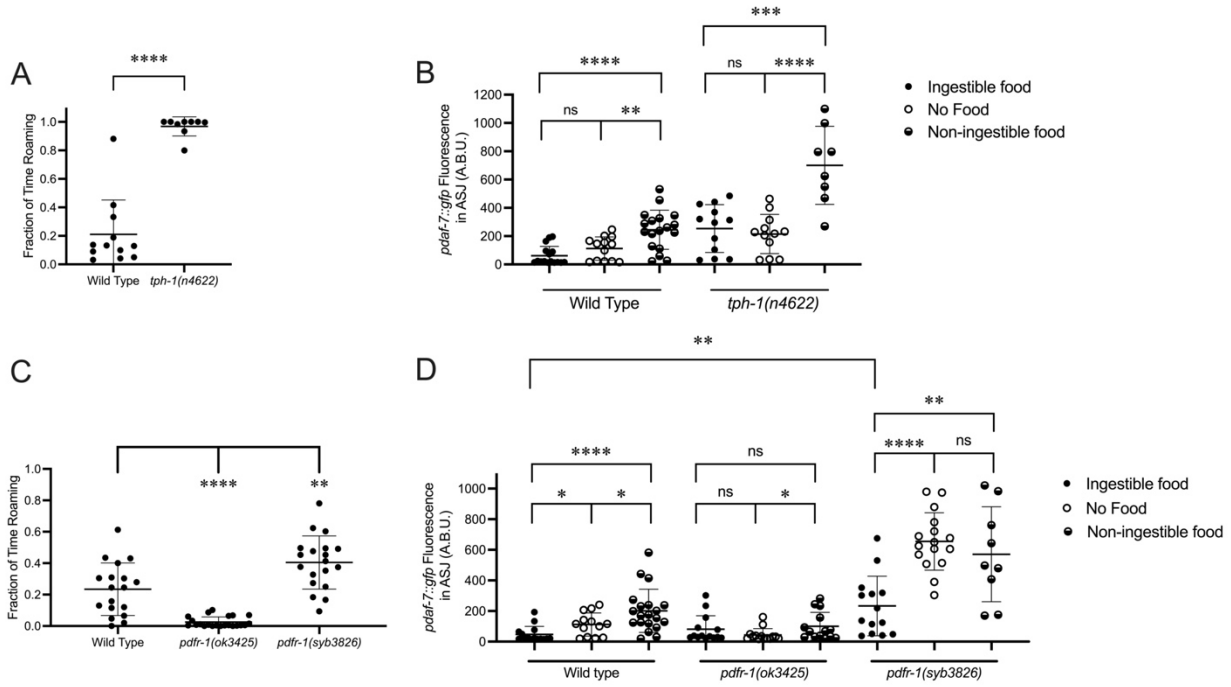

Figure 3. Known modulators of roaming and dwelling affect *daf-7* expression in the ASJ neurons

A. Fraction of time roaming of wild type and *tph-1(n4622)* animals. Each point represents an individual animal, and error bars indicate standard deviation. ****p<0.0001 as determined by an unpaired two-tailed t-test.

B. Maximum fluorescence values of *pdaf-7::gfp* in the ASJ neurons of adult wild type and *tph-1(n4622)* animals under "Fed," "Empty" and "Bottom" conditions. Each point represents an individual animal, and error bars indicate standard deviation. ****p<0.0001, ***p<0.001, **p<0.01, ns not signigivant as determined by an unpaired two-tailed t-test.

570 C. Fraction of time roaming of wild type, *pdfr-1(ok3425),* and *pdfr-1(syb3826)* animals.
571 Each point represents an individual animal, and error bars indicate standard deviation.
572 ****$p<0.0001$, **$p<0.01$ as determined by an unpaired two-tailed t-test.
573 D. Maximum fluorescence values of *pdaf-7::gfp* in the ASJ neurons of adult wild type, *pdfr-*
574 *1(ok3425),* and *pdfr-1(syb3826)* animals under "Fed," "Empty," and "Bottom"
575 conditions. Each point represents an individual animal, and error bars indicate standard
576 deviation. ****$p<0.0001$, **$p<0.01$, *$p<0.05$, ns not significant as determined by an
577 unpaired two-tailed t-test.

578

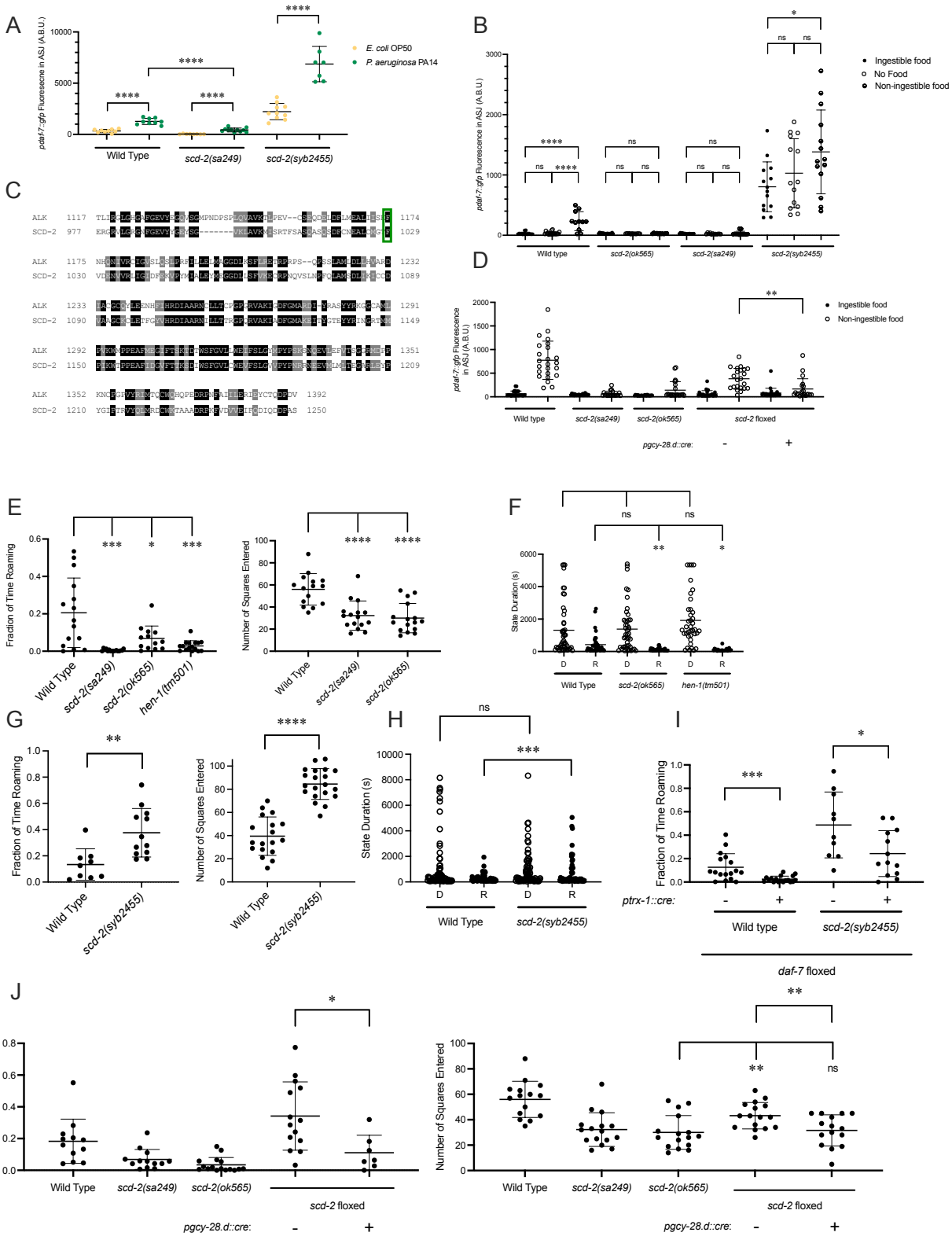
A
pdaf-7::gfp Fluorescence in ASJ (A.B.U.)
E. coli OP50
P. aeruginosa PA14
Wild Type
scd-2(sa249)
scd-2(syb2455)
B
pdaf-7::gfp Fluorescence in ASJ (A.B.U.)
Ingestible food
No Food
Non-ingestible food
Wild type
scd-2(ok565)
scd-2(sa249)
scd-2(syb2455)
C
ALK
SCD-2
D
pdaf-7::gfp Fluorescence in ASJ (A.B.U.)
Ingestible food
Non-ingestible food
Wild type
scd-2(sa249)
scd-2(ok565)
scd-2 floxed
pgcy-28.d::cre:
E
Fraction of Time Roaming
Number of Squares Entered
Wild Type
scd-2(sa249)
scd-2(ok565)
hen-1(tm501)
F
State Duration (s)
Wild Type
scd-2(ok565)
hen-1(tm501)
G
Fraction of Time Roaming
Number of Squares Entered
Wild Type
scd-2(syb2455)
H
State Duration (s)
Wild Type
scd-2(syb2455)
I
Fraction of Time Roaming
ptrx-1::cre:
Wild type
scd-2(syb2455)
daf-7 floxed
J
Fraction of Time Roaming
Number of Squares Entered
Wild Type
scd-2(sa249)
scd-2(ok565)
scd-2 floxed
pgcy-28.d::cre:

579

580 **Figure 4. SCD-2 regulates *daf-7* expression in the ASJ neurons and roaming behavior**

581 A. Maximum fluorescence values of *pdaf-7::gfp* in the ASJ neurons of adult wild type, *scd-*
582 *2(sa249),* and *scd-2(syb2455)* animals exposed to *E. coli* OP50 and *P. aeruginosa* PA14.
583 Each point represents an individual animal, and error bars indicate standard deviation.
584 ****p<0.0001, as determined by an unpaired two-tailed t-test.

585 B. Maximum fluorescence values of *pdaf-7::gfp* in the ASJ neurons of adult wild type, *scd-*
586 *2(ok565), scd-2(sa249),* and *scd-2(syb2455)* animals under "Fed," "Empty," and
587 "Bottom" conditions. Each point represents an individual animal, and error bars indicate
588 standard deviation. ****p<0.0001, *p<0.05, ns not significant as determined by an
589 unpaired two-tailed t-test. ****p<0.0001, *p<0.05 as determined by an unpaired two-
590 tailed t-test.

591 C. Sequence alignment of the kinase domains of human ALK (top) and *C. elegans* SCD-2
592 (bottom). Amino acids highlighted in black are identical and those in gray are similar.
593 F1174/F1029 is outlined in green.

594 D. Maximum fluorescence values of *pdaf-7::gfp* in the ASJ neurons of adult wild type,
595 floxed *scd-2, scd-2(sa249), scd-2(ok565),* and floxed *scd-2* animals with a transgene
596 expressing Cre under the AIA-specific *gcy-28.d* promoter under "Fed" and "Bottom"
597 conditions. Each point represents an individual animal, and error bars indicate standard
598 deviation. **p<0.01 as determined by an unpaired two-tailed t-test.

599 E. Fraction of time spent roaming (left) and number of squares entered in exploration assay
600 (right) for wild type, *scd-2(sa249), scd-2(ok565)* and *hen-1(tm501)* animals. Each point
601 represents an individual animal. Error bars indicate standard deviation. ****p<0.0001,
602 ***p<0.001, *p<0.05 as determined by an unpaired two-tailed t-test.

603 F. Duration of roaming (closed circles) and dwelling (open circles) states for wild type, *scd-*
604 *2(ok565)* and *hen-1(tm501*. Each point represents a discrete roaming or dwelling period.
605 Error bars indicate standard deviation. **p<0.01, *p<0.05, ns not significant as
606 determined by an unpaired two-tailed t-test.
607 G. Fraction of time spent roaming (left) and number of squares entered in exploration assay
608 (right) for wild type and *scd-2(syb2455)* animals. Each point represents an individual
609 animal. Error bars indicate standard deviation. ****p<0.0001, **p<0.01 as determined by
610 an unpaired two-tailed t-test.
611 H. Duration of roaming (closed circles) and dwelling (open circles) states for wild type and
612 *scd-2(syb2455)* animals. Each point represents a discrete roaming or dwelling period.
613 Error bars indicate standard deviation. ***p<0.001, ns not significant as determined by
614 an unpaired two-tailed t-test.
615 I. Fraction of time roaming for wild-type of *scd-2(syb2455)* animals with a floxed allele of
616 *daf-7* with or without an ASJ-specific cre transgene. ***p<0.001, *p<0.05 as determined
617 by an unpaired two-tailed t-test.
618 J. Left: Fraction of time spent roaming in worm tracker assay for *scd-2(sa249), scd-*
619 *2(ok565)* and floxed *scd-2* with or without a transgene expressing Cre under the AIA-
620 specific *gcy-28.d* promoter. Right: number of squares entered in exploration assay for
621 wild type, *scd-2(sa249), scd-2(ok565),* and floxed *scd-2* with or without a transgene
622 expressing Cre under the AIA-specific *gcy-28.d* promoter. Each point represents an
623 individual animal. Error bars indicate standard deviation. **p<0.01, *p<0.05, ns not
624 significant as determined by an unpaired two-tailed t-test.
625

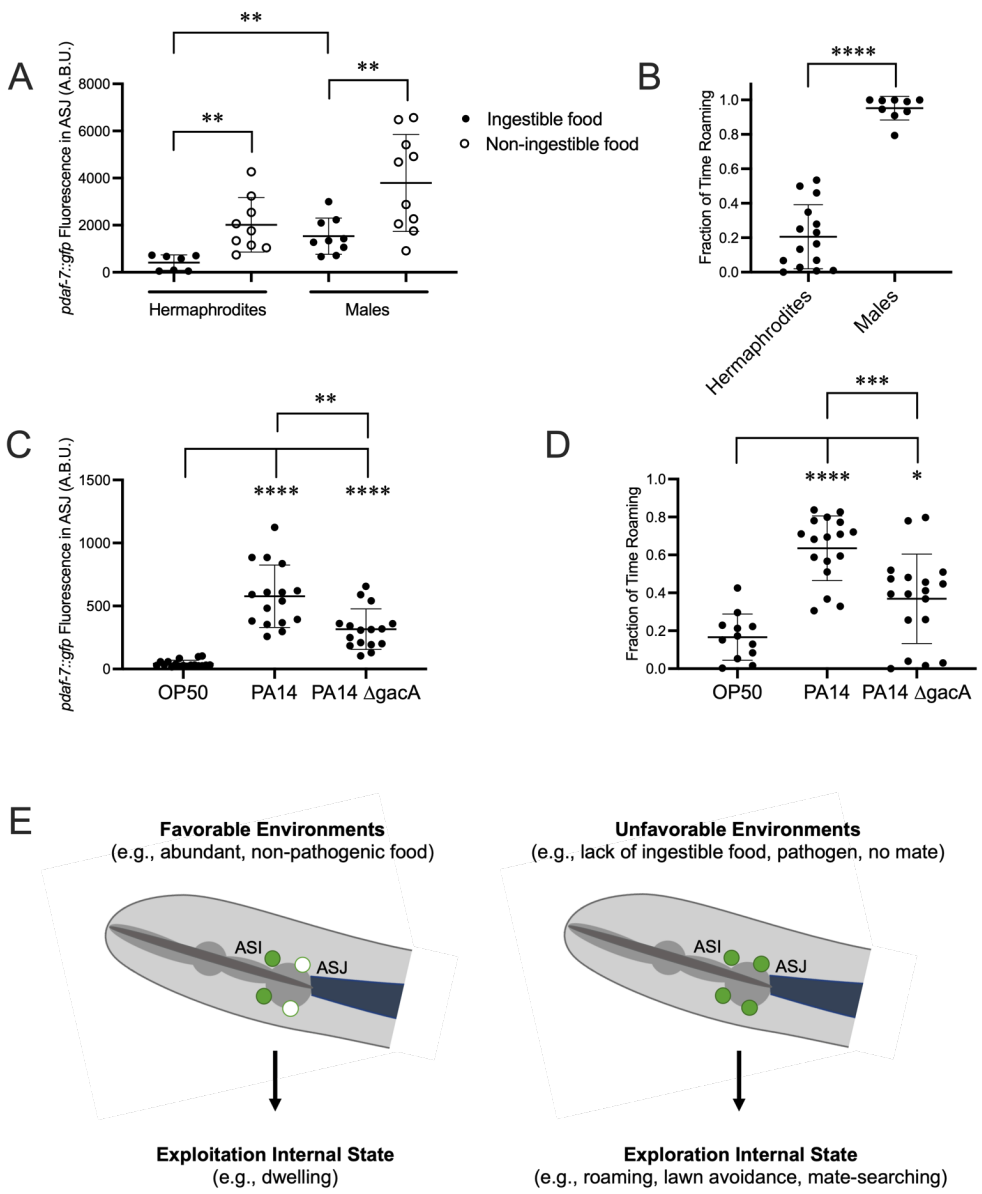

Figure 5. DAF-7 expression in the ASJ neurons correlates with an increase in roaming behavior under various conditions

A. Maximum fluorescence values of *pdaf-7::gfp* in the ASJ neurons of adult hermaphrodites and males under "Fed" and "Aztreonam" conditions. Each point represents an individual animal, and error bars indicate standard deviation. **p<0.01 as determined by an unpaired t-test.

633 B. Fraction of time roaming of wild-type hermaphrodites and males. Each point represents
634 an individual animal, and error bars indicate standard deviation. ****p<0.0001 as
635 determined by an unpaired t-test.
636 C. Maximum fluorescence values of *pdaf-7::gfp* in the ASJ neurons of adult hermaphrodites
637 fed *E. coli* OP50, *P. aeruginosa* PA14 or *P. aeruginosa* PA14ΔgacA. Each point
638 represents an individual animal, and error bars indicate standard deviation.
639 ****p<0.0001, **p<0.01 as determined by an unpaired t-test.
640 D. Fraction of time roaming of wild-type hermaphrodites on *E. coli* OP50, *P. aeruginosa*
641 PA14, or PA14 ΔgacA. Each point represents an individual animal, and error bars
642 indicate standard deviation. ****p<0.0001, ***p<0.001, *p<0.05 as determined by an
643 unpaired t-test.
644 E. *daf-7* expression in the ASJ neurons responds to environmental conditions and is
645 correlated with internal state. Under favorable conditions, *daf-7* is not expressed in the
646 ASJ neurons, and this is correlated with an internal state that favors exploitation of the
647 animal's current environment. Under unfavorable conditions, *daf-7* expression is induced
648 in the ASJ neurons, consistent with an internal state that favors exploration.

References

Bargmann, C. I. (2012). Beyond the connectome: how neuromodulators shape neural circuits. *Bioessays*, *34*(6), 458-465. https://doi.org/10.1002/bies.201100185

Ben Arous, J., Laffont, S., & Chatenay, D. (2009). Molecular and sensory basis of a food related two-state behavior in C. elegans. *PLoS One*, *4*(10), e7584. https://doi.org/10.1371/journal.pone.0007584

Boor, S. (2022). *Genetic Analysis of Bacterial Food Perception and its Influence on Foraging Behavior in C. elegans* Massachusetts Institute of Technology]. Cambridge, MA.

Brenner, S. (1974). The genetics of Caenorhabditis elegans. *Genetics*, *77*(1), 71-94. https://doi.org/10.1093/genetics/77.1.71

Chen, Y., Takita, J., Choi, Y. L., Kato, M., Ohira, M., Sanada, M., Wang, L., Soda, M., Kikuchi, A., Igarashi, T., Nakagawara, A., Hayashi, Y., Mano, H., & Ogawa, S. (2008). Oncogenic mutations of ALK kinase in neuroblastoma. *Nature*, *455*(7215), 971-974. https://doi.org/10.1038/nature07399

Cheng, L. Y., Bailey, A. P., Leevers, S. J., Ragan, T. J., Driscoll, P. C., & Gould, A. P. (2011). Anaplastic lymphoma kinase spares organ growth during nutrient restriction in Drosophila. *Cell*, *146*(3), 435-447. https://doi.org/10.1016/j.cell.2011.06.040

Churgin, M. A., McCloskey, R. J., Peters, E., & Fang-Yen, C. (2017). Antagonistic Serotonergic and Octopaminergic Neural Circuits Mediate Food-Dependent Locomotory Behavior in Caenorhabditis elegans. *J Neurosci*, *37*(33), 7811-7823. https://doi.org/10.1523/JNEUROSCI.2636-16.2017

Connolly, K. J. (1966). Locomotor activity in Drosophila as a function of food deprivation. *Nature*, *209*(5019), 224. https://doi.org/10.1038/209224a0

Dobosiewicz, M., Liu, Q., & Bargmann, C. I. (2019). Reliability of an interneuron response depends on an integrated sensory state. *Elife*, *8*. https://doi.org/10.7554/eLife.50566

Entchev, E. V., Patel, D. S., Zhan, M., Steele, A. J., Lu, H., & Ch'ng, Q. (2015). A gene-expression-based neural code for food abundance that modulates lifespan. *Elife*, *4*, e06259. https://doi.org/10.7554/eLife.06259

Flavell, S. W., Gogolla, N., Lovett-Barron, M., & Zelikowsky, M. (2022). The emergence and influence of internal states. *Neuron*, *110*(16), 2545-2570. https://doi.org/10.1016/j.neuron.2022.04.030

Flavell, S. W., Pokala, N., Macosko, E. Z., Albrecht, D. R., Larsch, J., & Bargmann, C. I. (2013). Serotonin and the neuropeptide PDF initiate and extend opposing behavioral states in C. elegans. *Cell*, *154*(5), 1023-1035. https://doi.org/10.1016/j.cell.2013.08.001

Flavell, S. W., Raizen, D. M., & You, Y. J. (2020). Behavioral States. *Genetics*, *216*(2), 315-332. https://doi.org/10.1534/genetics.120.303539

Franco, R., Rocco, G., Marino, F. Z., Pirozzi, G., Normanno, N., Morabito, A., Sperlongano, P., Stiuso, P., Luce, A., Botti, G., & Caraglia, M. (2013). Anaplastic lymphoma kinase: a glimmer of hope in lung cancer treatment? *Expert Rev Anticancer Ther*, *13*(4), 407-420. https://doi.org/10.1586/era.13.18

Fujiwara, M., Sengupta, P., & McIntire, S. L. (2002). Regulation of body size and behavioral state of C. elegans by sensory perception and the EGL-4 cGMP-dependent protein kinase. *Neuron*, *36*(6), 1091-1102. https://doi.org/10.1016/s0896-6273(02)01093-0

George, R. E., Sanda, T., Hanna, M., Frohling, S., Luther, W., 2nd, Zhang, J., Ahn, Y., Zhou, W., London, W. B., McGrady, P., Xue, L., Zozulya, S., Gregor, V. E., Webb, T. R., Gray, N. S., Gilliland, D. G., Diller, L., Greulich, H., Morris, S. W., . . . Look, A. T. (2008).

Activating mutations in ALK provide a therapeutic target in neuroblastoma. *Nature*, *455*(7215), 975-978. https://doi.org/10.1038/nature07397

Golden, J. W., & Riddle, D. L. (1982). A pheromone influences larval development in the nematode Caenorhabditis elegans. *Science*, *218*(4572), 578-580. https://doi.org/10.1126/science.6896933

Golden, J. W., & Riddle, D. L. (1984a). ACaenorhabditis elegans dauer-inducing pheromone and an antagonistic component of the food supply. *J Chem Ecol*, *10*(8), 1265-1280. https://doi.org/10.1007/BF00988553

Golden, J. W., & Riddle, D. L. (1984b). The Caenorhabditis elegans dauer larva: developmental effects of pheromone, food, and temperature. *Dev Biol*, *102*(2), 368-378. https://doi.org/10.1016/0012-1606(84)90201-x

Golden, J. W., & Riddle, D. L. (1984c). A pheromone-induced developmental switch in Caenorhabditis elegans: Temperature-sensitive mutants reveal a wild-type temperature-dependent process. *Proc Natl Acad Sci U S A*, *81*(3), 819-823. https://doi.org/10.1073/pnas.81.3.819

Greer, E. R., Perez, C. L., Van Gilst, M. R., Lee, B. H., & Ashrafi, K. (2008). Neural and molecular dissection of a C. elegans sensory circuit that regulates fat and feeding. *Cell Metab*, *8*(2), 118-131. https://doi.org/10.1016/j.cmet.2008.06.005

Gruninger, T. R., Gualberto, D. G., & Garcia, L. R. (2008). Sensory perception of food and insulin-like signals influence seizure susceptibility. *PLoS Genet*, *4*(7), e1000117. https://doi.org/10.1371/journal.pgen.1000117

Gutman, R., Yosha, D., Choshniak, I., & Kronfeld-Schor, N. (2007). Two strategies for coping with food shortage in desert golden spiny mice. *Physiol Behav*, *90*(1), 95-102. https://doi.org/10.1016/j.physbeh.2006.08.033

Hallberg, B., & Palmer, R. H. (2013). Mechanistic insight into ALK receptor tyrosine kinase in human cancer biology. *Nat Rev Cancer*, *13*(10), 685-700. https://doi.org/10.1038/nrc3580

Harris, N., Bates, S. G., Zhuang, Z., Bernstein, M., Stonemetz, J. M., Hill, T. J., Yu, Y. V., Calarco, J. A., & Sengupta, P. (2023). Molecular encoding of stimulus features in a single sensory neuron type enables neuronal and behavioral plasticity. *Curr Biol*, *33*(8), 1487-1501 e1487. https://doi.org/10.1016/j.cub.2023.02.073

Herbers, J. M. (1981). Time resources and laziness in animals. *Oecologia*, *49*(2), 252-262. https://doi.org/10.1007/BF00349198

Hilbert, Z. A., & Kim, D. H. (2017). Sexually dimorphic control of gene expression in sensory neurons regulates decision-making behavior in C. elegans. *Elife*, *6*. https://doi.org/10.7554/eLife.21166

Hilbert, Z. A., & Kim, D. H. (2018). PDF-1 neuropeptide signaling regulates sexually dimorphic gene expression in shared sensory neurons of C. elegans. *Elife*, *7*. https://doi.org/10.7554/eLife.36547

Holla, V. R., Elamin, Y. Y., Bailey, A. M., Johnson, A. M., Litzenburger, B. C., Khotskaya, Y. B., Sanchez, N. S., Zeng, J., Shufean, M. A., Shaw, K. R., Mendelsohn, J., Mills, G. B., Meric-Bernstam, F., & Simon, G. R. (2017). ALK: a tyrosine kinase target for cancer therapy. *Cold Spring Harb Mol Case Stud*, *3*(1), a001115. https://doi.org/10.1101/mcs.a001115

Inoue, T., & Thomas, J. H. (2000). Suppressors of transforming growth factor-beta pathway mutants in the Caenorhabditis elegans dauer formation pathway. *Genetics*, *156*(3), 1035-1046. https://doi.org/10.1093/genetics/156.3.1035

741 Ishihara, T., Iino, Y., Mohri, A., Mori, I., Gengyo-Ando, K., Mitani, S., & Katsura, I. (2002).
742 HEN-1, a secretory protein with an LDL receptor motif, regulates sensory integration and
743 learning in Caenorhabditis elegans. *Cell*, *109*(5), 639-649. https://doi.org/10.1016/s0092-
744 8674(02)00748-1
745 Iwahara, T., Fujimoto, J., Wen, D., Cupples, R., Bucay, N., Arakawa, T., Mori, S., Ratzkin, B.,
746 & Yamamoto, T. (1997). Molecular characterization of ALK, a receptor tyrosine kinase
747 expressed specifically in the nervous system. *Oncogene*, *14*(4), 439-449.
748 https://doi.org/10.1038/sj.onc.1200849
749 Janoueix-Lerosey, I., Lequin, D., Brugieres, L., Ribeiro, A., de Pontual, L., Combaret, V.,
750 Raynal, V., Puisieux, A., Schleiermacher, G., Pierron, G., Valteau-Couanet, D., Frebourg,
751 T., Michon, J., Lyonnet, S., Amiel, J., & Delattre, O. (2008). Somatic and germline
752 activating mutations of the ALK kinase receptor in neuroblastoma. *Nature*, *455*(7215),
753 967-970. https://doi.org/10.1038/nature07398
754 Ji, N., Madan, G. K., Fabre, G. I., Dayan, A., Baker, C. M., Kramer, T. S., Nwabudike, I., &
755 Flavell, S. W. (2021). A neural circuit for flexible control of persistent behavioral states.
756 *Elife*, *10*. https://doi.org/10.7554/eLife.62889
757 Johnson, R. E., Linderman, S., Panier, T., Wee, C. L., Song, E., Herrera, K. J., Miller, A., &
758 Engert, F. (2020). Probabilistic Models of Larval Zebrafish Behavior Reveal Structure on
759 Many Scales. *Curr Biol*, *30*(1), 70-82 e74. https://doi.org/10.1016/j.cub.2019.11.026
760 Kim, D. H., & Flavell, S. W. (2020). Host-microbe interactions and the behavior of
761 Caenorhabditis elegans. *J Neurogenet*, *34*(3-4), 500-509.
762 https://doi.org/10.1080/01677063.2020.1802724
763 Kyani-Rogers, T., Philbrook, A., McLachlan, I. G., Flavell, S. W., O'Donnell, M. P., &
764 Sengupta, P. (2022). Developmental history modulates adult olfactory behavioral
765 preferences via regulation of chemoreceptor expression in Caenorhabditiselegans.
766 *Genetics*, *222*(3). https://doi.org/10.1093/genetics/iyac143
767 Lipton, J., Kleemann, G., Ghosh, R., Lints, R., & Emmons, S. W. (2004). Mate searching in
768 Caenorhabditis elegans: a genetic model for sex drive in a simple invertebrate. *J*
769 *Neurosci*, *24*(34), 7427-7434. https://doi.org/10.1523/JNEUROSCI.1746-04.2004
770 McLachlan, I. G., Kramer, T. S., Dua, M., DiLoreto, E. M., Gomes, M. A., Dag, U., Srinivasan,
771 J., & Flavell, S. W. (2022). Diverse states and stimuli tune olfactory receptor expression
772 levels to modulate food-seeking behavior. *Elife*, *11*. https://doi.org/10.7554/eLife.79557
773 Meisel, J. D., Panda, O., Mahanti, P., Schroeder, F. C., & Kim, D. H. (2014). Chemosensation of
774 bacterial secondary metabolites modulates neuroendocrine signaling and behavior of C.
775 elegans. *Cell*, *159*(2), 267-280. https://doi.org/10.1016/j.cell.2014.09.011
776 Morris, S. W., Kirstein, M. N., Valentine, M. B., Dittmer, K. G., Shapiro, D. N., Saltman, D. L.,
777 & Look, A. T. (1994). Fusion of a kinase gene, ALK, to a nucleolar protein gene, NPM,
778 in non-Hodgkin's lymphoma. *Science*, *263*(5151), 1281-1284.
779 https://doi.org/10.1126/science.8122112
780 Oranth, A., Schultheis, C., Tolstenkov, O., Erbguth, K., Nagpal, J., Hain, D., Brauner, M.,
781 Wabnig, S., Steuer Costa, W., McWhirter, R. D., Zels, S., Palumbos, S., Miller Iii, D. M.,
782 Beets, I., & Gottschalk, A. (2018). Food Sensation Modulates Locomotion by Dopamine
783 and Neuropeptide Signaling in a Distributed Neuronal Network. *Neuron*, *100*(6), 1414-
784 1428 e1410. https://doi.org/10.1016/j.neuron.2018.10.024
785 Orthofer, M., Valsesia, A., Magi, R., Wang, Q. P., Kaczanowska, J., Kozieradzki, I., Leopoldi,
786 A., Cikes, D., Zopf, L. M., Tretiakov, E. O., Demetz, E., Hilbe, R., Boehm, A., Ticevic,

M., Noukas, M., Jais, A., Spirk, K., Clark, T., Amann, S., . . . Penninger, J. M. (2020). Identification of ALK in Thinness. *Cell*, *181*(6), 1246-1262 e1222. https://doi.org/10.1016/j.cell.2020.04.034

Overton, J. M., & Williams, T. D. (2004). Behavioral and physiologic responses to caloric restriction in mice. *Physiol Behav*, *81*(5), 749-754. https://doi.org/10.1016/j.physbeh.2004.04.025

Park, J., Meisel, J. D., & Kim, D. H. (2020). Immediate activation of chemosensory neuron gene expression by bacterial metabolites is selectively induced by distinct cyclic GMP-dependent pathways in Caenorhabditis elegans. *PLoS Genet*, *16*(8), e1008505. https://doi.org/10.1371/journal.pgen.1008505

Pradhan, S., Quilez, S., Homer, K., & Hendricks, M. (2019). Environmental Programming of Adult Foraging Behavior in C. elegans. *Curr Biol*, *29*(17), 2867-2879 e2864. https://doi.org/10.1016/j.cub.2019.07.045

Reiner, D. J., Ailion, M., Thomas, J. H., & Meyer, B. J. (2008). C. elegans anaplastic lymphoma kinase ortholog SCD-2 controls dauer formation by modulating TGF-beta signaling. *Curr Biol*, *18*(15), 1101-1109. https://doi.org/10.1016/j.cub.2008.06.060

Ren, P., Lim, C. S., Johnsen, R., Albert, P. S., Pilgrim, D., & Riddle, D. L. (1996). Control of C. elegans larval development by neuronal expression of a TGF-beta homolog. *Science*, *274*(5291), 1389-1391. https://doi.org/10.1126/science.274.5291.1389

Rhoades, J. L., Nelson, J. C., Nwabudike, I., Yu, S. K., McLachlan, I. G., Madan, G. K., Abebe, E., Powers, J. R., Colon-Ramos, D. A., & Flavell, S. W. (2019). ASICs Mediate Food Responses in an Enteric Serotonergic Neuron that Controls Foraging Behaviors. *Cell*, *176*(1-2), 85-97 e14. https://doi.org/10.1016/j.cell.2018.11.023

Russell, J. C., Epling, W. F., Pierce, D., Amy, R. M., & Boer, D. P. (1987). Induction of voluntary prolonged running by rats. *J Appl Physiol (1985)*, *63*(6), 2549-2553. https://doi.org/10.1152/jappl.1987.63.6.2549

Ryan, D. A., Miller, R. M., Lee, K., Neal, S. J., Fagan, K. A., Sengupta, P., & Portman, D. S. (2014). Sex, age, and hunger regulate behavioral prioritization through dynamic modulation of chemoreceptor expression. *Curr Biol*, *24*(21), 2509-2517. https://doi.org/10.1016/j.cub.2014.09.032

Sawin, E. R., Ranganathan, R., & Horvitz, H. R. (2000). C. elegans locomotory rate is modulated by the environment through a dopaminergic pathway and by experience through a serotonergic pathway. *Neuron*, *26*(3), 619-631. https://doi.org/10.1016/s0896-6273(00)81199-x

Schackwitz, W. S., Inoue, T., & Thomas, J. H. (1996). Chemosensory neurons function in parallel to mediate a pheromone response in C. elegans. *Neuron*, *17*(4), 719-728. https://doi.org/10.1016/s0896-6273(00)80203-2

Scheer, E., & Bargmann, C. I. (2023). Sensory neurons couple arousal and foraging decisions in C. elegans. *Elife*, *12:RP88657*. https://doi.org/https://doi.org/10.7554/eLife.88657.2

Sengupta, P. (2013). The belly rules the nose: feeding state-dependent modulation of peripheral chemosensory responses. *Curr Opin Neurobiol*, *23*(1), 68-75. https://doi.org/10.1016/j.conb.2012.08.001

Shaw, W. M., Luo, S., Landis, J., Ashraf, J., & Murphy, C. T. (2007). The C. elegans TGF-beta Dauer pathway regulates longevity via insulin signaling. *Curr Biol*, *17*(19), 1635-1645. https://doi.org/10.1016/j.cub.2007.08.058

832 Shinkai, Y., Yamamoto, Y., Fujiwara, M., Tabata, T., Murayama, T., Hirotsu, T., Ikeda, D. D.,
833 Tsunozaki, M., Iino, Y., Bargmann, C. I., Katsura, I., & Ishihara, T. (2011). Behavioral
834 choice between conflicting alternatives is regulated by a receptor guanylyl cyclase, GCY-
835 28, and a receptor tyrosine kinase, SCD-2, in AIA interneurons of Caenorhabditis
836 elegans. *J Neurosci*, *31*(8), 3007-3015. https://doi.org/10.1523/JNEUROSCI.4691-
837 10.2011
838 Wexler, L. R., Miller, R. M., & Portman, D. S. (2020). C. elegans Males Integrate Food Signals
839 and Biological Sex to Modulate State-Dependent Chemosensation and Behavioral
840 Prioritization. *Curr Biol*, *30*(14), 2695-2706 e2694.
841 https://doi.org/10.1016/j.cub.2020.05.006
842 White, J. G., Southgate, E., Thomson, J. N., & Brenner, S. (1986). The structure of the nervous
843 system of the nematode Caenorhabditis elegans. *Philos Trans R Soc Lond B Biol Sci*,
844 *314*(1165), 1-340. https://doi.org/10.1098/rstb.1986.0056
845 Wolfe, G. S., Tong, V. W., Povse, E., Merritt, D. M., Stegeman, G. W., Flibotte, S., & van der
846 Kooy, D. (2019). A Receptor Tyrosine Kinase Plays Separate Roles in Sensory
847 Integration and Associative Learning in C. elegans. *eNeuro*, *6*(4).
848 https://doi.org/10.1523/ENEURO.0244-18.2019
849 Woodling, N. S., Aleyakpo, B., Dyson, M. C., Minkley, L. J., Rajasingam, A., Dobson, A. J.,
850 Leung, K. H. C., Pomposova, S., Fuentealba, M., Alic, N., & Partridge, L. (2020). The
851 neuronal receptor tyrosine kinase Alk is a target for longevity. *Aging Cell*, *19*(5), e13137.
852 https://doi.org/10.1111/acel.13137
853 *WormLab*. In. (2020). MBF Bioscience.
854 Yap, E. L., & Greenberg, M. E. (2018). Activity-Regulated Transcription: Bridging the Gap
855 between Neural Activity and Behavior. *Neuron*, *100*(2), 330-348.
856 https://doi.org/10.1016/j.neuron.2018.10.013
857 Zaslaver, A., Liani, I., Shtangel, O., Ginzburg, S., Yee, L., & Sternberg, P. W. (2015).
858 Hierarchical sparse coding in the sensory system of Caenorhabditis elegans. *Proc Natl*
859 *Acad Sci U S A*, *112*(4), 1185-1189. https://doi.org/10.1073/pnas.1423656112
860